Science of the Total Environment 887 (2023) 163911

Contents lists available at ScienceDirect

Science of the Total Environment

journal homepage: www.elsevier.com/locate/scitotenv

Threat of soil formation rate to health of karst ecosystem

Chen Ran [a,b,c], Xiaoyong Bai [a,d,e,*], Qiu Tan [f], Guangjie Luo [e], Yue Cao [a,c,d], Luhua Wu [a,b,c], Fei Chen [a,g], Chaojun Li [a,b,c], Xuling Luo [a,c,f], Min Liu [a,c,f], Sirui Zhang [a,c,f]

[a] State Key Laboratory of Environmental Geochemistry, Institute of Geochemistry, Chinese Academy of Sciences, Guiyang 550081, Guizhou Province, China
[b] University of Chinese Academy of Sciences, Beijing 100049, China
[c] Puding Karst Ecosystem Observation and Research Station, Chinese Academy of Sciences, Puding 562100, Guizhou Province, China
[d] CAS Center for Excellence in Quaternary Science and Global Change, Xi'an 710061, Shanxi Province, China
[e] Guizhou Provincial Key Laboratory of Geographic State Monitoring of Watershed, Guizhou Education University, Guiyang 550018, China
[f] School of Geography and Environmental Sciences, Guizhou Normal University, Guiyang 550001, China
[g] College of Resources and Environmental Engineering, Guizhou University, Guiyang 550025, China

HIGHLIGHTS

- Soil formation rate is the key to restrict the karst ecosystem health.
- An optimized evaluation index system for karst ecosystem health was proposed.
- An 8 km × 8 km global karst ecosystem health index dynamic map is created.
- The proportion of unhealthy areas in the global karst ecosystem is as high as 75.91 %.

GRAPHICAL ABSTRACT

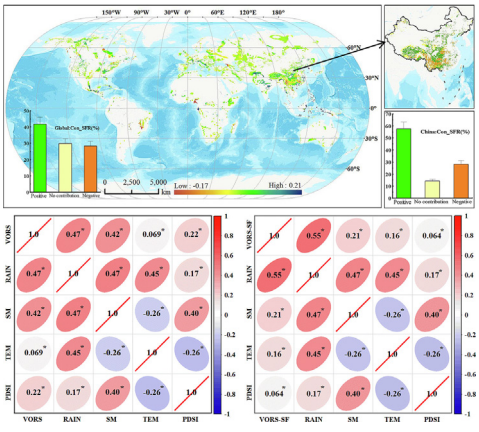

ARTICLE INFO

Editor: Charlotte Poschenrieder

Keywords:
Karst ecosystems
Soil formation rate
Ecosystem health
Global change
Driving factors

ABSTRACT

Karst ecosystems are important to several billion people, so it is necessary to accurately diagnose and evaluate the health of these ecosystems for socioeconomic development; however, the existing evaluation methods have many limitations, so they cannot accurately evaluate the ecosystem health in karst areas. In particular, they ignore the influence and restriction of the soil formation rate on the ecosystem health. To this end, we established a new index to represent the actual health status of karst ecosystems. The soil formation rate was found to pose a threat to the health of 28 % of the world's karst ecosystems, covering an area of 594 km^2. In addition, a dataset of global karst ecosystem health index values with a spatial resolution of about 8 km × 8 km from 2000 to 2014 was created, and the proportion of unhealthy areas was found to be as high as 75.91 %. This study highlights the contribution of the soil formation rate to karst ecosystem health and provides a new method and deeper scientific understanding for further accurate evaluation of karst ecosystem health, which can improve future ecosystem health research and social management.

* Corresponding author at: State Key Laboratory of Environmental Geochemistry, Institute of Geochemistry, Chinese Academy of Sciences, Guiyang 550081, Guizhou Province, China.
E-mail address: baixiaoyong@vip.skleg.cn (X. Bai).

http://dx.doi.org/10.1016/j.scitotenv.2023.163911
Received 27 November 2022; Received in revised form 28 April 2023; Accepted 29 April 2023
Available online 5 May 2023

1. Introduction

Healthy ecosystems are vital for global human survival and sustainable development (Peng et al., 2015; He et al., 2019), however, intensive human activities have greatly changed the structure and function of ecosystems owing to scientific and technological progress and the rapid growth of the global economy (Qiu et al., 2015; Bai et al., 2023). This has caused a variety of ecological and environmental problems, such as resource depletion, land desertification, soil erosion, and biodiversity reduction (Seto and Satterthwaite, 2010; de Groot et al., 2012). In the context of global change, karst ecosystems are of great importance owing to their fragility (Zhao et al., 2020), the diagnosis of karst ecosystem health is of great value and significance to realizing sustainable social development and the formulation of restoration strategies for degraded ecosystems.

The global karst area of 2200 × 10^4 km^2, accounting for 15 % of the Earth's total area, affects the survival and development of one billion people (Yuan, 1997). The fragile ecological environment in karst areas is closely related to the presence of less surface soil and serious vegetation and soil degradation caused by excessive human disturbance. In karst areas, the soil layer is thin and discontinuous (Wang, 2002; Sun et al., 2002a, 2002b. Once the soil is lost, rocky desertification will occur, which poses a serious threat to regional ecological environmental protection and social and economic development (Jiang et al., 2014; Zhang et al., 2021a; Zhang et al., 2021b). To promote ecosystem restoration and protection in karst areas, it is necessary to assess the ecosystem health.

Foreign research on ecosystem health has mostly focused on individual ecosystems (Bouyer et al., 2007; Rombouts et al., 2013; Ishtiaque et al., 2016; Madeira et al., 2018), or ecosystem health assessment has been combined with other topics to further explore its influencing factors and to provide a meaningful reference for social development (Keith et al., 2016; Fitch and Kim, 2018; Faridah-Hanuma et al., 2019; Marco et al., 2019). In karst areas, some scholars have used the fuzzy mathematics method, the ecological footprint model, the Pressure-State-Response (PSR) model, and various other research methods to study karst ecosystem health (Cao and Su, 2009; Zhang et al., 2011a, 2011b; Li et al., 2015; Liao et al., 2018), there are also a few scholars assessed the spatial and temporal changes in karst ecosystem health used the vigor-organization-resilience model (Lv et al., 2023; Xiao et al., 2022).

These studies are of great significance to the enrichment and improvement of ecosystem health theory. However, karst ecosystems differ from other ecosystems, that is, the soil is mainly derived from acid-insoluble substance (Wang, 1999; Sun et al., 2002a, 2002b; Wu and Qi, 2021), but the acid-insoluble substances in most karst areas account for <10 % of the total material, and pure limestone or dolomite accounts for <1 %, leading to slow soil formation in karst areas. The time required to form a 1 m thick soil layer from a pure carbonate matrix is 250–7800 ka, which is 10–40 times that in non-karst areas (Cao et al., 2003; Ma and Zhang, 2018). Therefore, the soil formation rate, as a key limiting factor in karst ecosystems (Zhang et al., 2021c), is a problem that we must consider when studying the health of karst ecosystems. Moreover, previous studies have mostly focused on small areas, single ecosystems, or single watersheds. There is no set of standard systems suitable for ecosystem health evaluation in karst areas, and the driving factors affecting karst ecosystem health and the prediction of future scenarios remain unclear.

In this study, we investigated the importance of the soil formation rate for karst ecosystem health assessment, and we combined the soil formation rate (SFR) and the vigor, organization, resilience, and services model to establish a suitable ecosystem health diagnosis model for karst areas. The spatial and temporal patterns and future trends of global karst ecosystem health were further clarified, and the key factors influencing ecosystem health were identified. The results of this study link ecosystem health with soil environmental characteristics and geochemical processes. These results provide valuable information for the assessment of ecosystem health in karst areas and also provide a theoretical basis for the formulation of degraded ecosystem restoration strategies.

2. Materials and methods

2.1. Data sources

The data used in the study included the global karst boundary, Land Use (2000–2015), Normalized Difference Vegetation Index (NDVI), Rainfall, Evapotranspiration, Temperature, Soil moisture and Palmer Drought Severity Index (PDSI). More details about these variables were provided as Table S1.

2.2. Methods

2.2.1. The thermodynamic dissolution equilibrium model for carbonate zones

Based on the internationally universal thermodynamic dissolution equilibrium model (White, 1984) given in (1), Gombert (2002) created a model for estimating the theoretical maximum annual dissolution rate of carbonate rocks, see Eq. (2), what this model expresses is: Assume that the carbonate rocks have been exposed to air for a long time, under the current climate and hydrological characteristics, the carbonate dissolution effect has reached a state of equilibrium. Analyze the theoretical activity of Ca^{2+} ions or HCO_3^- ions under the current hydrological and climate background in the dissolution equilibrium of $CaCO_3$ to reflect the dissolution of carbonate rocks. Based on the above, the theoretical consumption of atmospheric CO_2 is inverted (Gaillardet et al., 1999; Zeng et al., 2016).

$$CaCO_3 + CO_2 + H_2O \Leftrightarrow Ca^{2+} + 2HCO_3^- \tag{1}$$

$$\begin{aligned} D_{\max} &= 10^6 (P - E)[Ca_{2+}]_{eq} \\ &= 10^6 (P - E)\left(K_s K_1 K_0 / 4 K_2 \gamma_{(Ca^{2+})^3}\right)^{1/3} (pCO_2)^{1/3} \end{aligned} \tag{2}$$

where, D_{max} is the potential maximum dissolution rate of carbonate rock, P, E is the total rainfall and evapotranspiration respectively. K_s is the calcite solubility constant, K_1 is the equilibrium constant of CO_2 hydration and dissociation as HCO_3^-, K_0 is the equilibrium constant of CO_2 in water, K_2 is the equilibrium constant for CO_3^{2-}. $\gamma_{Ca^{2+}}$ and $\gamma_{HCO_3^-}$ are the activity coefficients of Ca^{2+} and HCO_3^- ions in water. ρCO_2 is the partial pressure of CO_2 in soil or aquifer, ρCO_2 is calculated from Brook's formula (Brook et al., 1983) as follows:

$$\log(\rho CO_2) = -3.47 + 2.09 \times \left(1 - e^{-0.00172E}\right) \tag{3}$$

K_s, K_1, K_2, and K_0 are calculated according to formulas (4), (5), (6) and (7):

$$\log(K_s) = A + B \times T_k + C/T_k + D \times \log(T_k) \tag{4}$$

$$\log(K_1) = A + B \times T_k + C/T_k + D \times \log(T_k) + E/T_k^2 \tag{5}$$

$$\log(K_2) = A + B \times T_k + C/T_k + D \times \log(T_k) + E/T_k^2 \tag{6}$$

$$\log(K_0) = A + B/T_k + C \times T_k \tag{7}$$

where, T_k is the Kelvin temperature, and A–E is the calculation coefficient corresponding to K_i factor (Plummer and Busenberg, 1982; Gombert, 2002), and the parameters are shown in the Table 1.

The ionic activity coefficients of Ca^{2+} and HCO_3^- are calculated by the Debye-Hückel equation (Plummer and Busenberg, 1982), see in formula (8).

$$\log(\gamma_i) = -AZ_i^2 \frac{\sqrt{I}}{1 + Ba_i\sqrt{I}} \tag{8}$$

where, γ_i represents the ionic activity coefficient of ion i, a_i is the ionic radius (Ca^{2+} radius is 6A, HCO_3^- radius is 4A) (Dreybrodt, 1988), Z_i is the

Table 1
Coefficients of the formulas for the K_i factors.

	A	B	C	D	E
K_s	−171.9065	−0.077993	2839.3191	71.595	–
K_1	−356.3094	−0.06091964	21,834.37	126.8339	−1,684,915
K_2	−107.8871	−0.03252849	5151.79	38.92561	−563,713.9
K_0	−14.0184	2385.73	0.015264	–	–

number of ionic charge, I is the ionic strength, A and B depend on the Celsius temperature T (°C), the calculation method is:

$$A = 0.4883 + 8.074 \times 10^{-4}T \quad (9)$$

$$B = 0.3241 + 1.6 \times 10^{-4}T \quad (10)$$

$$I = \frac{1}{2}\Sigma_i Z_i^2 C_i \quad (11)$$

where C_i is the ionic concentration (mol L^{-1}).

$$SFR = D_{max} Q_\rho P + R(1 - P) \quad (12)$$

where D_{max} is the Carbonate rocks dissolution rate (mm/yr, Converted to $m^3\ km^{-2}\ yr^{-1}$), Q is the acid insoluble content (%); P is the carbonate content (%); ρ is the Carbonate bulk density (t/m^3); R is the Soil formation rate of non-carbonate rocks ($t\ km^{-2}\ yr^{-1}$).

2.2.2. Assessment of karst ecosystem health

The ecosystem health of the ecosystem space entity reflects the ability to maintain a healthy structure, self-regulation and recovery under pressure, and can be divided into three categories: Ecosystem Vigor (EV), Ecosystem Organization (EO) and Ecosystem Resilience (ER) (Costanza, 1992; Pantus and Dennision, 2005; Ran et al., 2021). The study is based on assessment indicators of ecosystem health, combined with Ecosystem Services (ES) (Peng et al., 2015; He et al., 2019) and Soil Formation Rate (SFR), to evaluate global karst ecosystem health. The Ecosystem Health Index (EHI) is expressed as:

$$EHI(VORS\_SFR) = \sqrt[5]{EV \times EO \times ER \times ES \times SFR}$$

In this paper, the normalized difference vegetation index is selected as the vigor index because it is closely related to net primary productivity (Xie et al., 2021), it is an effective indicator for monitoring regional or global vegetation and the ecological environment (Li et al., 2017a, 2017b; Li et al., 2020a, 2020b), widely used to refer to an ecosystem vigor index (Phillips et al., 2008; Costanza, 2012a, 2012b; Peng et al., 2017; Liao et al., 2018).

Ecosystem organization refers to the stability of the ecosystem structure (Peterson, 2002; Costanza, 2012a, 2012b), and the landscape pattern index is used to measure the heterogeneity and connectivity of the landscape (Turner, 1989; Howell et al., 2018). The weighted aggregation method is used to calculate the EO index (Ran et al., 2021), the weights of the patch connectivity index of Landscape Heterogeneity (LH), Landscape Connectivity (LC) and important ecological functions (IC) are 0.35, 0.35 and 0.30, respectively (Frondoni et al., 2011; Peng et al., 2015; Kang et al., 2018). The EO is calculated as follows:

$$\begin{aligned} EO &= 0.35LH + 0.35LC + 0.30IC \\ &= (0.25SHID + 0.10AWMPFD) + (0.25FN + 0.10CONT) + (0.07FN1 \\ &\quad + 0.03COHESION1 + 0.07FN2 + 0.03COHESION2 + 0.07FN3 \\ &\quad + 0.03COHESION3) \end{aligned}$$

where SHDI represents Shannon diversity index; AWMPFD refers to the area weighted average patch fractal dimension index; FN refers to Landscape fragmentation index; CONT refers to Landscape contagion index; FN_1, FN_2, FN_3 and $COHESION_1$, $COHESION_2$, $COHESION_3$ represent the Landscape fragmentation index and patch cohesion index of forest, water and grassland respectively. All indices involved in the EO calculation formula were calculated using landscape pattern software Fragstats 3.3.

Ecosystem resilience refers to the ability of natural ecosystems to restore their original structure and functions after being disturbed by external sources (Peng et al., 2015), a healthy ecosystem possesses adequate resilience to survive various small-scale perturbations, the Ecosystem Resilience Coefficient (ERC) was obtained by referring to existing research (Peng et al., 2017; Kang et al., 2018). The ER is calculated as follows:

$$ER = \sum_{i=1}^{n} Ai \times ERCi$$

where Ai represents the area ratio of land use types; $ERCi$ represents the ERC of land use type i; n is the number of land use types.

Ecosystem service function refers to the capacity of ecosystem to provide goods and services for human society (He et al., 2019). The study identified forest land as the land use type with the most ecosystem service value (Gong et al., 2013; Peng et al., 2015), and calculated the Relative Ecosystem Service Coefficient (RESC) based on forest land, with a threshold of [0,1] (Dobbs et al., 2011; Peng et al., 2015), as shown in Table S2. In addition, referring to the existing literature, the coefficient of the spatial proximity effect of land use type on ecosystem services is calculated through a coefficient matrix (Marulli and Mallarach, 2005). The calculation formula of ES is as follows:

$$ES = \sum_{j=1}^{m} RESC_j \times \left(1 + \frac{CSNE_j}{100}\right)/m$$

where $RESC_j$ is the RESC of the land use type related to the pixel j; $CSNE_j$ is the sum of the spatial proximity effect coefficients of the four adjacent pixels on the ecosystem service of the pixel j; m is the number of evaluation spatial entities of the pixel.

2.2.3. Theil-Sen median trend analysis and Mann-Kendall test

Theil-Sen median trend analysis is combined with Mann-Kendall test to determine the trend of long-term series data (Jiang et al., 2015; Chen et al., 2022; Xiong et al., 2022), Theil-Sen Median trend analysis is a robust nonparametric statistical trend calculation method that can reduce the impact of data outliers (Sen, 1968; Yang et al., 2019), the calculation formula is as follows:

$$\beta M = Median\left(\frac{M_j - M_i}{j - i}\right) \quad (2000 \le i \le j \le 2014)$$

where β_M is the median of the slope of n(n-1)/2 data combinations, when $\beta_M > 0$, it means that the change trend of the independent variable M during the study period is increasing, and vice versa.

Mann-Kendall is a non-parametric test method used to determine the significance of a trend and are not affected by abnormal values (Fensholt et al., 2012; Li et al., 2017a, 2017b). The formulas are as follows:

Set the $\{M_i\}, i = 2000, 2001, \ldots, 2014$, define the Z statistic as:

$$Z = \begin{cases} \dfrac{S-1}{\sqrt{\mathrm{var}(S)}}, S>0 \\ 0, S = 0 \\ \dfrac{S+1}{\sqrt{\mathrm{var}(S)}}, S < 0 \end{cases}$$

$$S = \Sigma_{j=1}^{n-1} \Sigma_{i=j+1}^{n} \operatorname{sgn}\left(M_j - M_i\right)$$

$$\operatorname{sgn}\left(M_j - M_i\right) = \begin{cases} 1, M_j - M_i > 0 \\ 0, M_j - M_i = 0 \\ -1, M_j - M_i < 0 \end{cases}$$

$$\operatorname{var}(S) = \frac{n(n-1)(2n+5)}{18}$$

In the formula, M_i and M_j are the pixel average values of variable M in the i-th and j-th years, n is the length of the year, and sgn is the sign function.

2.2.4. Contribution of soil formation rate to ecosystem health

Decompose changes in EHI into changes in the components of vigor, organization, resilience, service, and soil formation rate (Roderick et al., 2007; You et al., 2013), this method is widely used to evaluate the influence of various interference factors on hydrometeorological changes (Liu and Sun, 2016; Xiao et al., 2023; Li et al., 2022).

$$\frac{d_{EHI}}{dt} = \frac{d_{EV}}{dt} \cdot \frac{\partial_{EHI}}{\partial_{EV}} + \frac{d_{EO}}{dt} \cdot \frac{\partial_{EHI}}{\partial_{EO}} + \frac{d_{ER}}{dt} \cdot \frac{\partial_{EHI}}{\partial_{ER}} + \frac{d_{ES}}{dt} \cdot \frac{\partial_{EHI}}{\partial_{ES}} + \frac{d_{SFR}}{dt} \cdot \frac{\partial_{EHI}}{\partial_{SFR}} = Con\_EV + Con\_EO + Con\_ER + Con\_ES + Con\_SFR$$

Here, $\frac{d_{EHI}}{dt}$ refers to the Changing trend of *EHI*, *Con_EV*, *Con_EO*, *Con_ER*, *Con_ES*, *Con_SFR* refer to the contribution of *EV*, *EO*, *ER*, *ES*, *SFR* to *EHI*, respectively, $\frac{\partial_{EHI}}{\partial_{EV}}$, $\frac{\partial_{EHI}}{\partial_{EO}}$, $\frac{\partial_{EHI}}{\partial_{ER}}$, $\frac{\partial_{EHI}}{\partial_{ES}}$, $\frac{\partial_{EHI}}{\partial_{SFR}}$ represent the partial correlation coefficient between *EHI* and each variable, respectively. When calculating the partial correlation coefficient of each variable, it is assumed that other variables remain unchanged on their long-term average. According to the formula definition, the influence of the other four variables is eliminated, which is equivalent to the fourth-order partial correlation corresponding to each variable coefficient (Sun et al., 2019), the formula is as follows:

$$R_{SFR \cdot EHI\_EV \cdot EO \cdot ER \cdot ES} = \frac{R_{SFR \cdot EHI\_EV \cdot EO \cdot ER} - R_{SFR \cdot ES\_EV \cdot EO \cdot ER} \cdot R_{EHI \cdot ES\_EV \cdot EO \cdot ER}}{\sqrt{\left(1 - R^2_{SFR \cdot ES\_EV \cdot EO \cdot ER}\right)\left(1 - R^2_{EHI \cdot ES\_EV \cdot EO \cdot ER}\right)}}$$

In the formula, $R_{SFR \cdot EHI\_EV \cdot EO \cdot ER \cdot ES}$ represents the partial correlation coefficient of SFR to EHI after eliminating the influence of *EV*, *EO*, *ER* and *ES*; $R_{SFR \cdot EHI\_EV \cdot EO \cdot ER}$, $R_{SFR \cdot ES\_EV \cdot EO \cdot ER}$ and $R_{EHI \cdot ES\_EV \cdot EO \cdot ER}$ are defined as same as $R_{SFR \cdot EHI\_EV \cdot EO \cdot ER \cdot ES}$. In addition, the *t*-test is used to judge the significance of the correlation between two variables, if p is <0.05, the 95 % confidence significance test is passed, otherwise it is not significant.

2.2.5. CA-Markov prediction model

The CA-Markov model is a prediction method based on the Markov chain, which predicts the future changes of events based on their current state (Sang et al., 2011). Each grid in the distribution pattern of ecosystem health level is simulated as a cell, and the ecosystem health level type of each cell is the state of the cell. Based on the data of factors that affect ecosystem health, such as ecosystem vigor, organization, resilience, services, and soil formation rate, and apply the Logistic module in IDRISI software to obtain a suitability distribution atlas, the simulation operation is completed under the module in CA-Markov, so as to realize the simulation prediction of the spatial pattern change of the ecosystem health level.

The expression of Markov transition matrix is as follows:

$$s_{ij} = \begin{bmatrix} s_{11} & s_{12} & \cdots & s_{1n} \\ s_{21} & s_{22} & \cdots & s_{2n} \\ \vdots & \vdots & \ddots & \vdots \\ s_{n1} & s_{n2} & \cdots & s_{nn} \end{bmatrix}$$

$$p_{ij} = \begin{bmatrix} p_{11} & p_{12} & \cdots & p_{1n} \\ p_{21} & p_{22} & \cdots & p_{2n} \\ \vdots & \vdots & \ddots & \vdots \\ p_{n1} & p_{n2} & \cdots & p_{nn} \end{bmatrix}$$

where S means area; P means probability; $i, j (i, j = 1, 2, \cdots, n)$ represents each factor layer before and after transfer, respectively. Probability of each factor layer s_i to s_j is $p(s_i \rightarrow s_j) = p(s_i | s_j) = p_{ij}$.

2.2.6. Precision validation

The key to simulation prediction is the correctness of its prediction results. Kappa coefficient is often used to evaluate the accuracy of remote sensing data classification and analyze the consistency of two maps (Foody, 2006; Halmy et al., 2015), the closer the Kappa coefficient is to 1, the higher the simulation prediction accuracy (Mondal et al., 2016). The evaluation criteria (Feinstein and Cicchetti, 1990; Cicchetti and Feinstein, 1990) are shown in Table S3.

2.3. Statistical analysis

In this study, the data management tool (resample) was used to unify all of the data to a resolution of 0.5°. The dimensions of each evaluation index in the index system of the ecosystem health evaluation model are different, even when they have the same dimensions, and their actual numbers are also very different. To eliminate the influence caused by the different dimensions and the different quantities, it was necessary to standardize each index used in the comprehensive evaluation. First, the extreme value normalization method was used to uniformly normalize each index to the range of 0–1. Then, based on the isometric classification method, the indicators of the ecosystem health were divided into five levels: degradation (0–0.2), unhealthy (0.2–0.4), moderately healthy (0.4–0.6), sub-healthy (0.6–0.8), and most healthy (0.8–1.0).

In addition, combining Theil-Sen median trend analysis and Mann-Kendall test, reveals the change trend of the soil formation rate and ecosystem health indicators in the global carbonate rock region from 2000 to 2014, refer to existing research and classify them according to the change characteristics of each index: the area with $S \geq 0.0005$ is an increasing area, the area with $-0.0005 < S < 0.0005$ is a constant area, and the area with $S \leq -0.0005$ is a decreasing area. Using Mann-Kendall test (confidence level of 0.05), the results are divided into significant changes ($Z \geq 1.96$ or $Z \leq -1.96$) and insignificant changes ($-1.96 < Z < 1.96$), based on the above classification standards, the change trend of each index is finally divided into five levels: significant decrease, slight decrease, basically unchanged, slight increase and significant increase (Table S4).

3. Results

3.1. Spatial distribution pattern and change of global carbonate SFR

The SFR is affected by regional climate and hydrogeological conditions (Bai and Dent, 2009; Zeng et al., 2017; Li et al., 2018; Li et al., 2020a, 2020b), and its spatial distribution pattern exhibits significant regional differences (Fig. 1a). We found that the high SFR values were mainly distributed in the equatorial region. This region is characterized by high temperatures, abundant rainfall, and high humidity all year round, which promotes the dissolution of carbonate rocks, that is, it increases the dissolution rate of carbonate rocks, so the SFR is higher. The low SFR value areas were mainly distributed in several relatively arid and cold places, such as on plateaus; in the deserts in Central Asia, East Africa, and South Africa; and in the cold regions in the Northern Hemisphere. This was easily revealed through statistical analysis of the annual average SFR at different latitudes (Fig. 1b).

In this study, Theil-Sen median trend analysis and the Mann-Kendall test (Fig. S1) were used to analyze the change trend of the soil formation rate in carbonate regions around the world. The results show that (Fig. 2)

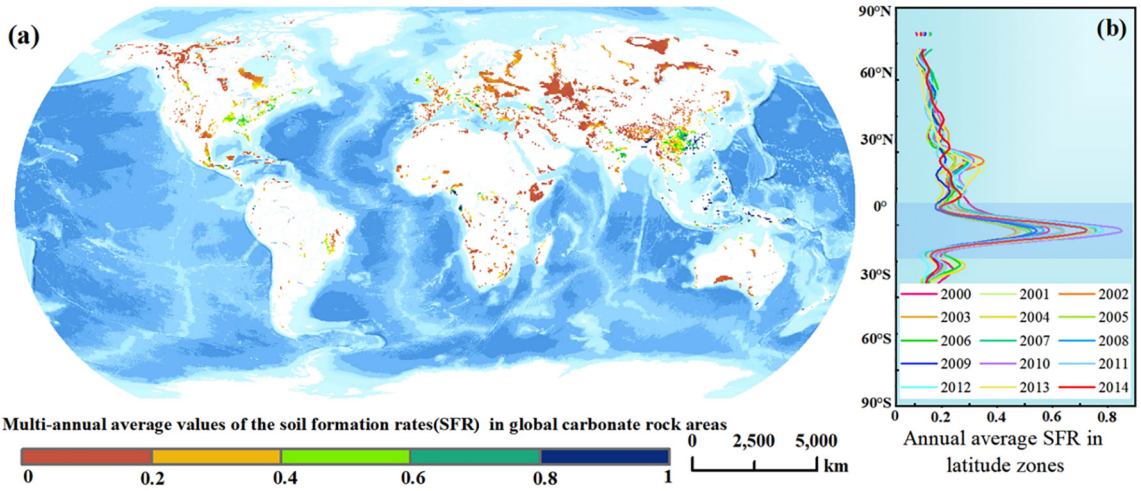

Fig. 1. Annual average SFR in the global carbonate region from 2000 to 2014.

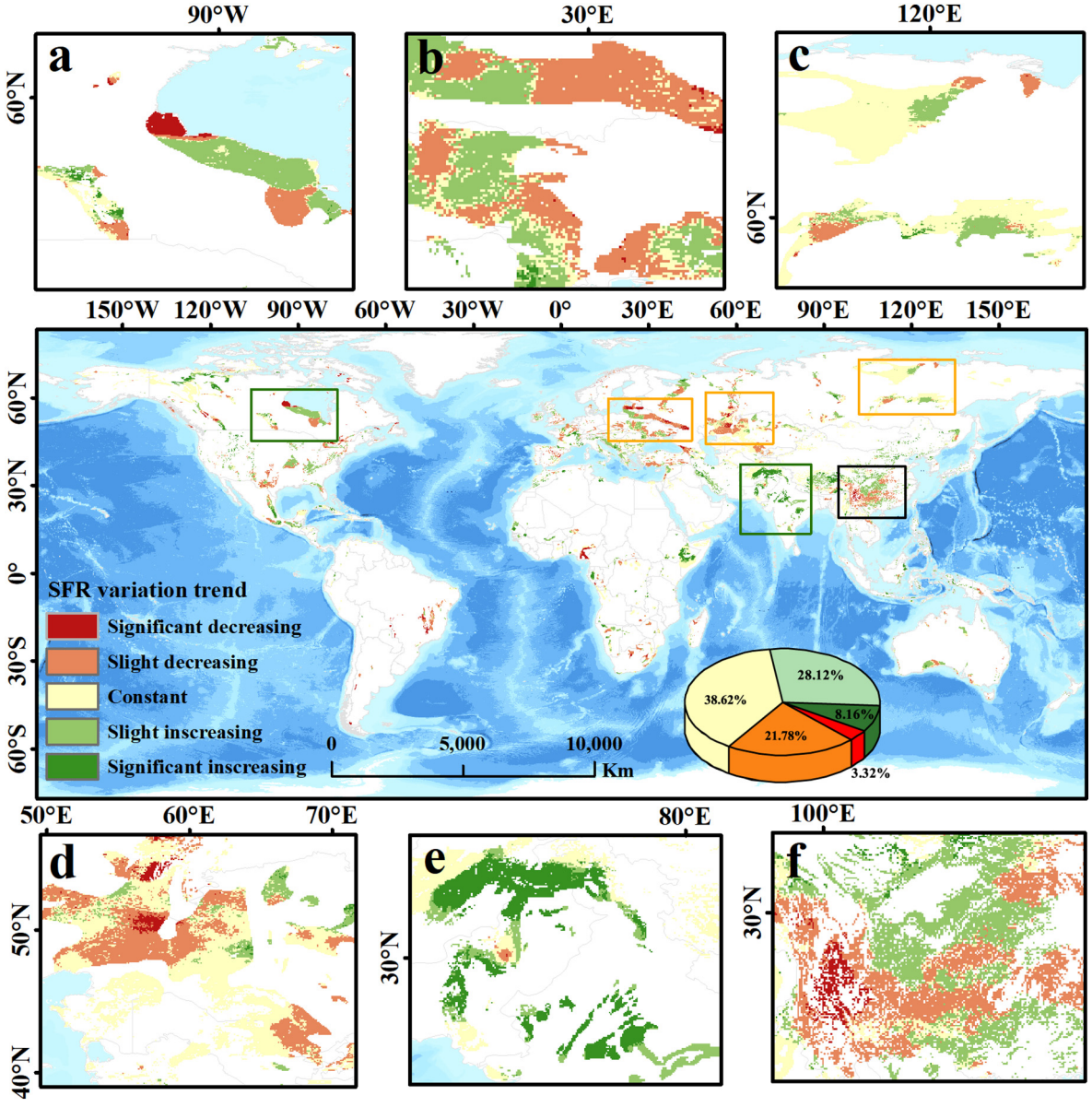

Fig. 2. Change trend of the SFR in the global carbonate region from 2000 to 2014.

the area where the soil formation rate remains basically unchanged accounted for the largest proportion (38.62 %), followed by the areas with a slight increase (28.12 %) and slight decrease (21.78 %). The areas with significant increases accounted for 8.16 %, and the areas with significant decreases accounted for 3.32 %. In general, the area in which the soil formation rate increased (36.28 %) was greater than the area in which it decreased (25.1 %).

In addition, according to the trend analysis of the SFR (Fig. 2), the areas with increased SFR values were mainly distributed on the coastal plain of Hudson Bay (Fig. 2a), in the Carpathian Mountains (Fig. 2b), near the Ganges River, on the Iranian Plateau (Fig. 2e), near the Yunnan-Guizhou Plateau, and in the Hengduan Mountains (Fig. 2f). We also found that the areas where the SFR decreased were mainly located west of the Dnieper River (Fig. 2b) and East of the Ural River (Fig. 2d). The areas where the SFR remained basically unchanged were mainly concentrated on the northeastern part of the Central Siberian Plateau (Fig. 2c), as well as in other scattered areas.

3.2. Contribution of SFR to ecosystem health

Carbonate rocks weathering is an important soil formation mechanism for developing soil resources in the karst areas in southern China (Wang, 1999), and it is also a true soil formation mechanism (Xu et al., 2005). The severity of soil erosion in karst areas largely depends on the rate of soil formation under the background of a specific geological environment (Li et al., 2006). The congenital insufficiency of the soil-forming materials provided by the carbonate rocks in karst areas leads to a slow SFR, and the bedrock can even be bare and lacking soil flow (Yuan, 1988). this leads to serious ecological disasters. Therefore, in karst areas, the impact of the soil formation rate cannot be ignored. In addition, through correlation analysis, it was found that the Pearson correlation coefficient between the soil formation rate and the ecosystem health index is positive (Fig. S2). The correlation coefficient between them is larger than the ecosystem organization with autocorrelation in the formula itself, indicating that the soil formation rate has a certain impact on the ecosystem health index. To further support this argument, we selected 13 regions around the world where karst is more concentrated and contiguous for analysis (Jiang et al., 2020). The average value of the ecosystem health obtained via statistical analysis of the rate of the added SFR and the non-added SFR in each region (Fig. 3) shows that the addition of the soil formation rate reduces the level of ecosystem health in each region. In each selected karst area, when the SFR is not considered, the ecosystem health is overestimated by >90 %, indicating that the SFR has a significant impact on the spatial variation in the ecosystem health. When the SFR is included in ecosystem health assessment, more comprehensive results can be obtained, helping to assess the ecosystem health more systematically, especially in karst areas that are extremely affected by SFR, and illustrating the importance of the SFR in karst ecosystem health assessment.

To further explore the impact of the soil formation rate on ecosystem health, the remaining four factors in the control model were held constant, and we calculated their partial correlation coefficients to obtain a spatial distribution map of the contribution of the soil formation rate to the ecosystem health (Fig. 4). In 42 % of the global karst areas, the SFR contributes positively to the ecosystem health; and in 28 % of the global karst areas, it contributes negatively. China is the country with the largest karst area and the widest distribution. Its karst area exceeds 1/3 of the land area (Song et al., 2017). The SFR makes a positive contribution to the ecosystem health in 57 % of this region, and it makes a negative contribution in about 28 %. It can be seen that the SFR mainly makes a positive contribution to the karst ecosystem health.

3.3. Karst ecosystem health diagnosis based on SFR

Taking into account the limiting effect of the soil formation rate on the ecosystem health in the carbonate rock area, we incorporated this factor into the ecosystem health calculation model to evaluate the ecosystem health status in the global carbonate rock area from 2000 to 2014 (Fig. S3). We found that during the study period, the high global multi-year average ecosystem health values were mainly distributed in the equatorial region with some high values in humid climate zones with good rainfall conditions (Fig. S3a), such as in Southwestern China, the Eastern European Plain, and the Western Siberian Plain. In addition, through statistical analysis of the ecosystem health index in the different latitude regions around the world over many years (Fig. S3b), it was found that the ecosystem health index has a clear advantage in the equatorial region throughout the year. In addition, in the low latitude regions (15–25°N) and in another higher value, high latitude region (50–65°N), at a given latitude range, the ecosystem health index in the Southern Hemisphere is much lower than that in the Northern Hemisphere. There is no peak between 15°N and 25°S, and the ecosystem health in the Southern Hemisphere above 25°S exhibits low values. Based on the climate and hydrological characteristics of the distribution areas of the ecosystem health index, we infer that this may be the main reason for the difference in the ecosystem health index.

3.4. Threat of soil formation rate to health of karst ecosystems

3.4.1. Simulation and prediction of future karst ecosystem health

Using the conversion rules established using the transition matrix of the ecosystem health grades from 2000 to 2015 based on the Markov model simulation (Cao et al., 2019), taking 2000 and 2015 as the starting years, and based on the cellular automats (CA)-Markov model, the distribution patterns of the ecosystem health index in 2015 and 2030 were simulated to obtain prediction maps of the ecosystem health in 2015 and 2030 (Fig. 5). The proportions of the actual calculated and predicted values in the different ecosystem health levels in the global carbonate rock regions in 2015 were basically the same, and their spatial distributions were also very similar, indicating that the predicted results have a certain reliability. By 2030, except for the areas where the ecosystem health level degraded, exhibiting a downward trend (1.76 %) compared to 2015, the ecosystem health levels of the other areas all exhibit an increasing state. In general, in 2030, the areas with relatively healthy levels (suboptimal health and highest health) (11.41 %) will increase by 0.87 % compared to 2015 (10.54 %). The areas with below average health levels (degraded and unhealthy) (73.29 %) will be 1.72 % smaller than in 2015 (75.01 %). Therefore, we expect the ecosystem health of the global carbonate rock area to gradually improve in the next 8 years.

To verify the accuracy of the calculation results of the CA-Markov model, we calculated the kappa coefficient of the calculated and simulated values of the ecosystem health level in 2015. The overall kappa coefficient was 0.9029. The kappa coefficient of each ecosystem health level is presented in Table 2. According to the classification standard of the kappa coefficient, the prediction results and calculation results of the ecosystem health in this study are better in 2030, indicating that the results obtained using the prediction model are highly reliable.

3.4.2. Threat of soil formation rate to health of karst ecosystems

As was discussed above, we predicted the health status of the global karst ecosystems in the future without taking into account the soil formation rate (Fig. S4). When the soil formation rate was not included in the ecosystem health diagnostic index system, in 2030, the area where the ecosystem health level will have degraded will be comparable to that in 2015. It will decrease by 11.5 %, and the areas of the remaining health levels will all increase (Fig. S4). In general, in 2030, the areas with relatively healthy levels (suboptimal health and highest health) (23.79 %) will have increased by 6.38 % compared to 2015 (17.41 %), and 62.08 % of the area will be below the average health level (degraded and unhealthy), which is 6.45 % less than in 2015 (68.53 %) (Fig. S4). Therefore, regardless of whether the soil formation rate is included in the ecosystem health diagnostic index system, the prediction results indicate that the ecosystem health of the global carbonate rock area will gradually improve in the next 8 years.

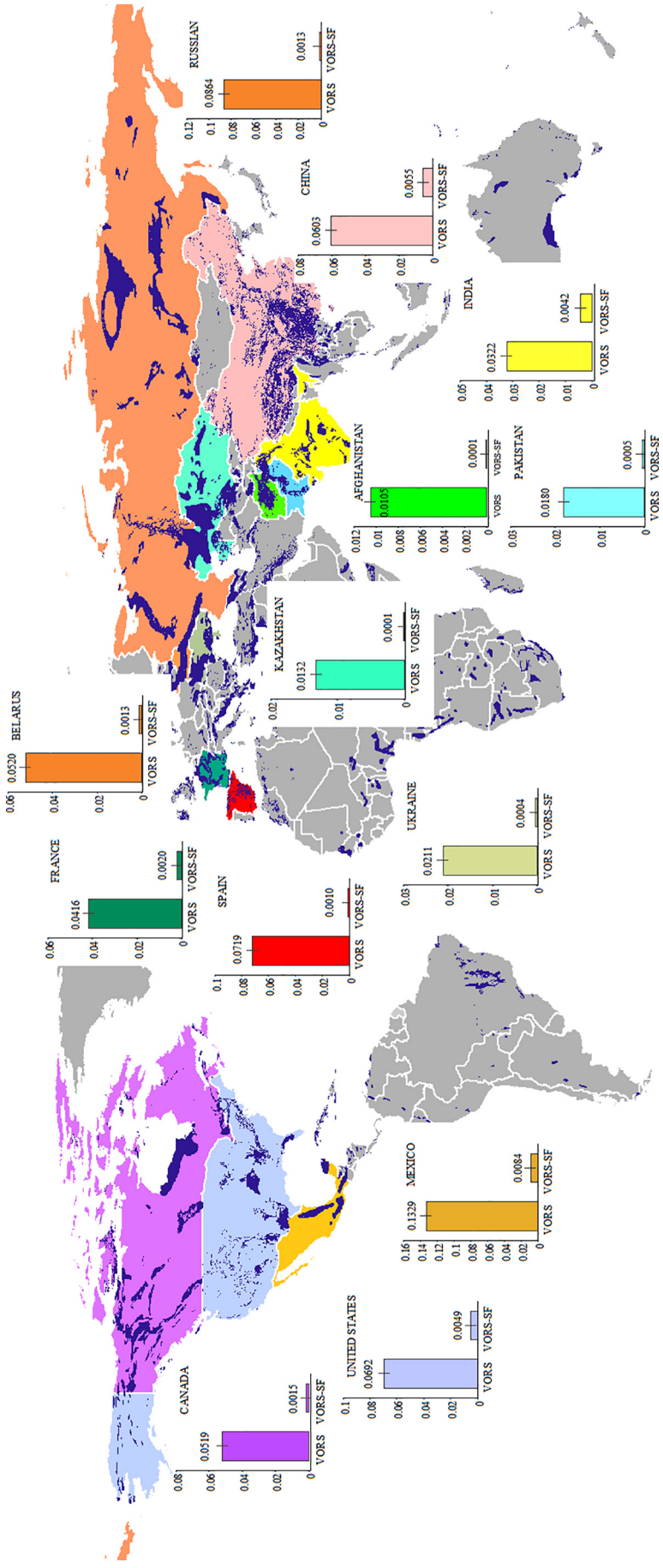

Fig. 3. Locations of the selected 13 contiguous karst areas and the average statistics of their levels of ecosystem health.

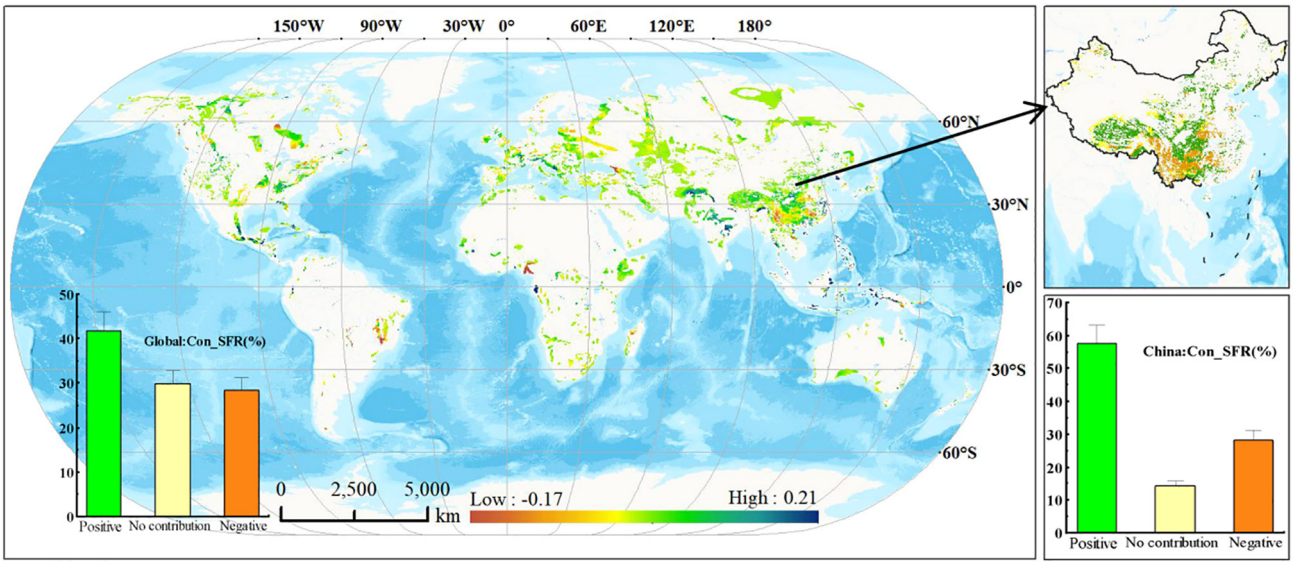

Fig. 4. Spatial distribution of the contribution of the soil formation rate to ecosystem health.

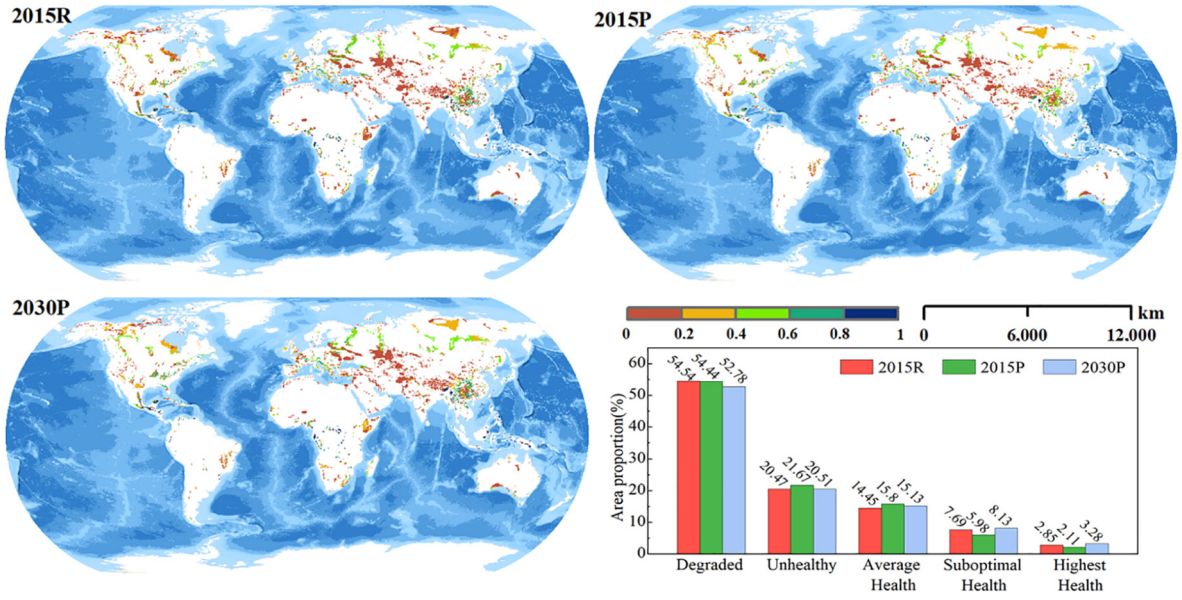

Fig. 5. Ecosystem health predictions and statistics of area proportions in 2015 and 2030 (R denotes the actual calculated results, and P denotes the prediction results).

Although our research results show that the ecosystem health of the global carbonate rock regions will gradually improve in the future, we found that when the soil formation rate is included in the ecosystem health diagnostic index system, the healthier regions will be more healthy in 2030 than in 2015, increasing by 0.87 %. The increase when the soil formation rate is not included (6.38 %) is 7.3 times that when it is. The area with a below average health level will decrease by 1.72 % compared to 2015, and the reduction when the soil formation rate is not included (6.45 %) is 3.75 times that when it is (Fig. S4). The ecosystem health index that takes into account the soil formation rate has a much lower degree of recovery than when it is not taken into account. Thus, it is concluded that the soil formation rate may limit the health of karst ecosystems.

Table 2
Kappa coefficient test value.

Real calculation results	Prediction results	Kappa
0–0.2	0–0.2	0.9726
0.2–0.4	0.2–0.4	0.8633
0.4–0.6	0.4–0.6	0.8120
0.6–0.8	0.6–0.8	0.5684
0.8–1	0.8–1	0.6255
Overall	–	0.9029

4. Discussion

4.1. Influence of SFR on the correlation between climatic conditions and ecosystem health

Through analysis of the temporal and spatial distributions of the various ecosystem health indicators in carbonate regions around the world, the spatial distributions and change trends of the various indicators were found to be largely restricted by the regional climate and hydrological conditions. In view of this, we analyzed the correlations between the regional climate and hydrological parameters and the ecosystem health. Based on the correlation diagram of the factors affecting the ecosystem health in carbonate rock regions (Fig. 6), we found that regardless of the additive soil rate, the average annual rainfall (r^2 = 0.47, 0.55) and soil moisture (r^2 = 0.42, 0.47) were

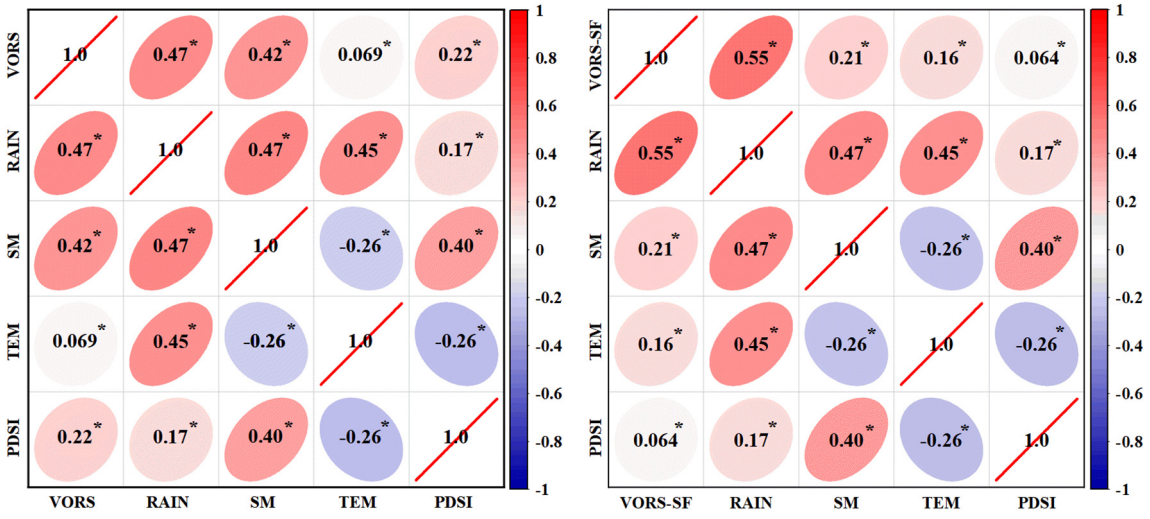

Fig. 6. Correlation diagram of the factors affecting the ecosystem health in carbonate rock regions.

the dominant factors affecting the regional heterogeneity of the ecosystem health within the global carbonate region.

Similar studies have shown that climatic factors have an impact on the provision of ecosystem services (Lorencová et al., 2016; Zhang et al., 2018; Bai et al., 2019), and it is the main determinant to regional ecological sensitivity (Zhang and Xu, 2017). Pan et al. (2020) et al. concluded that future climate change, mainly changes in rainfall and temperature, will have a significant impact on ecosystem health. These factors mainly affect the overall level of ecosystem health by affecting the ecosystem vigor (Cao and Woodward, 1998; Reeves et al., 2014). He et al. (2019) et al. explored the regional differences in ecosystem health in China and their driving factors, and they concluded that the moisture index is the main factor affecting the regional heterogeneity of the ecosystem health across China. In addition, we observed that the addition of the soil formation rate enhanced the correlations between the rainfall and temperature and the ecosystem health index and weakened the correlations between the drought index and soil moisture and the ecosystem health index.

4.2. Methodological advantages of considering the SFR in ecosystem health assessment

Here, we mainly describe the evolution of ecosystem health diagnostic model from proposal to improvement, and then explain the reasons and advantages of taking soil formation rate as the improvement of ecosystem health diagnostic model in karst area. There are large differences in the range of indicators involved in the development of an ecosystem health assessment index (Bertollo, 1998; Costanza and Mageau, 1999; Costanza, 2012a, 2012b).

Costanza and Mageau (1999) proposed the VOR model constructed using three indicators, i.e., vigor (V), organization (O), and resilience (R), which has been widely recognized by the ecological community (Wang et al., 2018; Xiao et al., 2019). Many ecosystem health assessment studies on different scales have been conducted using this model. Later, a large number of scholars improved the ecosystem health assessment model on this basis, and they concluded that including ecosystem services can enable a better and more comprehensive evaluation of ecosystem health (Yan et al., 2016). Therefore, the VORS model gradually replaced the VOR model.

The VORS model has an excellent universality and also provides a good method of ecosystem health assessment; however, it is precisely because of the universality of this model that researchers commonly ignore the regional differences caused by the geological background. The weathering of carbonate rock is the most basic and common geological and geochemical process in carbonate rock areas (Zhang et al., 2011a, 2011b). It is also the main form of rock-soil-water-atmosphere-biological interactions in karst areas and is a key link in the epigenetic geochemical cycles of elements (Wang et al., 2019). The soil formation rate in the carbonate rock area is too slow, and soil formation is generally considered to be most significant over geological rather than human timescales (Green et al., 2019). This leads to a series of ecological and environmental problems. Therefore, the model established in this study is aimed at carbonate rock regions, and the limiting factor of the soil formation rate is added to the original model, which makes the ecosystem health assessment model more comprehensive and more targeted.

4.3. Uncertainty

There are many uncertainties in this study. The first source of uncertainty is the determination of the weight of each indicator. The weights of the indicators in this study were mainly obtained from the existing literature, so they have a certain degree of uncertainty. However, as a widely used model, the determination of the weights is relatively reliable. Second, the calculation of the index of the soil formation rate included in this study was based on the chemical weathering of carbonate rocks and acid-insoluble matter. The soil sources that were not considered included dust deposition out of the atmosphere, the influence of microbial action on rock formation and older alluvial-colluvial profiles covering the carbonate and forming deep oxisoils and so on. Studies have shown that there are many microorganisms on the surfaces of carbonate rocks, and the action of these microorganisms is involved throughout the weathering and evolution of carbonate rocks (Williams and Steinbergs, 1959). Microbes can even accelerate the dissolution of and soil formation from carbonate rocks (Zhang and Yuan, 2005; Ding and Lian, 2008). Alluvial-colluvial deposits are usually composed of materials such as sand, silt, and clay that have been transported and deposited by rivers or landslides. Over time, weathering and erosion processes can transform these deposits into oxisoils, which are highly weathered and infertile soils.

In addition, the uncertainty of our research is similar to the uncertainty in the study of Pengjian et al. As is explained by the special attention to landscape patterns in the assessment model, the results of the ecosystem health assessment are greatly affected by land use changes, and there is inevitable uncertainty in the interpretation of remote sensing images (Peng et al., 2015). Thus, when evaluating units with large spatial heterogeneity on the regional scale, there are obvious uncertainties in quantifying the ecosystem services for inclusion in the global average of each land use type.

Despite the unavoidable limitations in the data acquisition and methodology described above, we believe that this research is still meaningful. The results of this research can help researchers understand the spatial pattern of karst ecosystem health changes and their influencing factors and provide scientific support for the formulation of regional ecological protection and

restoration policies. Modern data collection conditions are superior, and the most obvious limitation of the ecosystem health assessment is not the lack of data but how the data on multiple assessment indicators are used to develop a suitable framework. Therefore, in this study on ecosystem health assessment, we considered integrating the indicators related to the environment, society, economy, and resources to make the ecosystem health assessment more comprehensive and specific.

5. Conclusions

Assessing the health of regional ecosystems is the basis for exploring the ecological impact of global environmental changes, and it is also important for the comprehensive analysis of the coupling mechanism between humans and nature. In this study, the SFR and the VORS model were combined to establish an ecosystem health diagnosis model suitable for karst regions, a preliminary diagnosis of the ecosystem health of global karst areas was conducted, future scenario simulation predictions were made, and the impact of the soil formation rate on the ecosystem health assessment was investigated. The main conclusions of this study are as follows.

(1) During the study period, the high values of multi-year average karst ecosystem health were mainly distributed in the equatorial region with humid climate zones with good rainfall conditions.
(2) The SFR and the VORS model were combined to simulate and predict the health of the global karst ecosystem in the future, it is expected that it will gradually improve in the next 8 years.
(3) The average annual rainfall ($r^2 = 0.47$) and soil moisture ($r^2 = 0.42$) are the main driving factors of the changes in the karst ecosystem health, and the addition of the SFR enhanced the correlations between the rainfall ($R^2 = 0.55$) and soil moisture ($R^2 = 0.47$) and the karst ecosystem health index.

The combination of the SFR and the VORS model provides a new research method for karst ecosystem health assessment research. This model is aimed at carbonate rock regions. Adding the limiting factor of the soil formation rate is added to the original model not only made the ecosystem health assessment model more comprehensive, but it also made it more targeted.

CRediT authorship contribution statement

C.R. and X.B. designed the study. C.R. collected the data. C.R. and X.B. analyzed the data. C.R., X.B., Q.T., G.L, Y.C., L.W., F.C., C.L., X.L., M.L. and S.Z. contributed significantly to the writing of the manuscript.

Data availability

Data will be made available on request.

Declaration of competing interest

The authors declare no competing interests.

Acknowledgements

This research work was supported by Joint Foundation of National Natural Science Foundation (No. U22A20619), Western Light Cross-team Program of Chinese Academy of Sciences (No. xbzg-zdsys-202101), National Natural Science Foundation of China (No. 42077455 & No. 42167032), Strategic Priority Research Program of the Chinese Academy of Sciences (No. XDB40000000 & No. XDA23060100), Guizhou Provincial Science and Technology Projects (No. Qiankehe Support [2022] General 198), High-level innovative talents in Guizhou Province (No. GCC[2022]015-1 & No. 2016-5648), Guizhou Provincial 2020 Science and Technology Subsidies (No. GZ2020SIG), Opening Fund of the State Key Laboratory of Environmental Geochemistry (No. SKLEG2022206 & No. SKLEG2022208), Central Government Leading Local Science and Technology Development (No. QianKeZhongYinDi [2021]4028).

Appendix A. Supplementary data

Supplementary data to this article can be found online at https://doi.org/10.1016/j.scitotenv.2023.163911.

References

Bai, X.Y., Zhang, S.R., Li, C.J., et al., 2023. A carbon-neutrality-capacity index for evaluating carbon sink contributions. Environ. Sci. Ecotechnology, 100237 https://doi.org/10.1016/j.ese.2023.100237.
Bai, Y., Ochuodho, T.O., Yang, J., 2019. Impact of land use and climate change on water-related ecosystem services in Kentucky, USA[J]. Ecol. Indic. 102, 51–64. https://doi.org/10.1016/j.ecolind.2019.01.079.
Bai, Z.G., Dent, D., 2009. Recent land degradation and improvement in China. Ambio 38, 150–156. https://doi.org/10.1579/0044-7447-38.3.150.
Bertollo, P., 1998. Assessing ecosystem health in governed landscapes: a framework for developing core indicators[J]. Ecosyst. Health 4 (1), 33–51. https://doi.org/10.1046/j.1526-0992.1998.00069.x 1998.
Bouyer, J., Sana, Y., Samandoulgou, Y., et al., 2007. Identification of ecological indicators for monitoring ecosystem health in the trans-boundary W regional park: a pilot study[J]. Biol. Conserv. 138 (1–2), 73–88. https://doi.org/10.1016/j.biocon.2007.04.001.
Brook, G.A., Folkoff, M.E., Box, E.O., 1983. A world model of soil carbon dioxide. Earth Surf. Process. Landf. 8, 79–88. https://doi.org/10.1002/esp.3290080108.
Cao, H., Su, W.C., 2009. Studies on ecosystem health evaluation based on fuzzy mathematics method in Karst Areas[J]. Res. Soil Water Conserv. 16 (03), 148–154 https://doi.org/CNKI:SUN:STBY.0.2009-03-033.
Cao, J.H., Yuan, D.X., Pan, X.G., 2003. Soil in karst ecosystems[J]. Adv. Earth Science 18 (1), 37–44.. https://kns.cnki.net/kcms/detail/detail.aspx?FileName=DXJZ200301006&DbName=CJFQ2003.
Cao, M.K., Woodward, F.I., 1998. Net primary and ecosystem production and carbon stocks of terrestrial ecosystems and their responses to climate change[J]. Glob. Chang. Biol. 4 (2), 185–198. https://doi.org/10.1046/j.1365-2486.1998.00125.x.
Cao, Y., Wang, S.J., Bai, X.Y., Li, H.W., et al., 2019. Spatial-temporal evolution processes and simulation of future soil erosion scenario in the karst valley of southern China[J]. Acta Ecol. Sin. 39 (16), 6061–6071. https://doi.org/10.5846/stxb201903300618.
Chen, F., Bai, X.Y., Liu, F., et al., 2022. Analysis long-term and spatial changes of Forest cover in typical karst areas of China[J]. Land 11 (8), 1349. https://doi.org/10.3390/land11081349.
Cicchetti, D.V., Feinstein, A.R., 1990. High agreement but low kappa:II.Resolving the paradoxes. J. Clin. Epidemiol. 43 (6), 551–558. https://doi.org/10.1016/0895-4356(90)90159-M.
Costanza, R., 1992. Towards an operational definition of health. In: Costanza, R., Norton, B., Haskell, B.D. (Eds.), Ecosystem Health—New Goals for Ecosystem Management. Inland Press, Washington, DC , pp. 239–256.. https://www.researchgate.net/publication/313508675_Toward_an_operational_definition_of_ecosystem_health/citation/download.
Costanza, R., 2012a. Ecosystem health and ecological engineering. Ecol. Eng. 45, 24–29. https://doi.org/10.1016/j.ecoleng.2012.03.023.
Costanza, R., 2012b. Ecosystem health and ecological engineering[J]. Ecol. Eng. 45 (8), 24–29. https://doi.org/10.1016/j.ecoleng.2012.03.023.
Costanza, R., Mageau, M., 1999. What is a healthy ecosystem?[J]. Aquat. Ecol. 33 (1), 105–115.
de Groot, Rudolf, Brander, Luke, van der Ploeg, Sander, et al., 2012. Global estimates of the value of ecosystems and their services in monetary units[J]. Ecosyst. Serv. 1 (1), 50–61. https://doi.org/10.1016/j.ecoser.2012.07.005.
Ding, L.J., Lian, B., 2008. Experimentation of microbial weathering to CaCO3[J]. Carsologica Sin. 27 (3), 197–200. https://doi.org/10.3969/j.issn.1001-4810.2008.03.001.
Dobbs, C., Escobedo, F.J., Zipperer, W.C., 2011. A framework for developing urban forest ecosystem services and goods indicators. Landsc. Urban Plan. 99 (3–4), 196–206. https://doi.org/10.1016/j.landurbplan.2010.11.004.
Dreybrodt, W., 1988. Processes in Karst Systems. Springer, Berlin, Heidelberg https://doi.org/10.1007/978-3-642-83352-6.
Faridah-Hanuma, I., Yusoff, F.M., Fitrianto, A., et al., 2019. Original articles development of a comprehensive mangrove quality index (MQI) in matang mangrove: assessing mangrove ecosystem health[J]. Ecol. Indic. 102, 103–117. https://doi.org/10.1016/j.ecolind.2019.02.030.
Feinstein, A.R., Cicchetti, D.V., 1990. High agreement but low kappa:i.The problems of two paradoxes. J. Clin. Epidemiol. 43 (6), 543–549. https://doi.org/10.1016/0895-4356(90)90158-L.
Fensholt, R., Langanke, T., Rasmussen, K., Reenberg, A., Prince, S.D., Tucker, C., et al., 2012. Greenness in semi-arid areas across the globe 1981–2007-an earth observing satellite based analysis of trends and drivers. Remote Sens. Environ. 121, 144–158. https://doi.org/10.1016/j.rse.2012.01.017.
Fitch, R.A., Kim, Y.S., 2018. Incorporating ecosystem health and fire resilience within the unified economic model of fire program analysis[J]. Ecol. Econ. 149 (7), 98–104. https://doi.org/10.1016/j.ecolecon.2018.02.017.
Foody, G.M., 2006. What is the difference between two maps: a remote senser's view[J]. J. Geogr. Syst. 8 (2), 119–130. https://doi.org/10.1007/s10109-006-0023-z.
Frondoni, R., Mollo, B., Capotorti, G., 2011. A landscape analysis of land cover change in the Municipality of Rome (Italy): spatio-temporal characteristics and ecological implications

of land cover transitions from 1954 to 2001. Landsc. Urban Plan. 100 (1–2), 117–128. https://doi.org/10.1016/j.landurbplan.2010.12.002.
Gaillardet, J., Dupre, B., Louvat, P., Allegre, C.J., 1999. Global silicate weathering and CO2 consumption rates deduced from the chemistry of large rivers. Chem. Geol. 159, 3–30. https://doi.org/10.1016/S0009-2541(99)00031-5.
Gombert, P., 2002. Role of karstic dissolution in global carbon cycle[J]. Glob. Planet. Chang. 33 (1–2), 177–184. https://doi.org/10.1016/S0921-8181(02)00069-3.
Gong, C.F., Yu, S.X., Joesting, H., et al., 2013. Determining socioeconomic drivers of urban forest fragmentation with historical remote sensing images[J]. Landsc. Urban Plan. 117 (9), 57–65. https://doi.org/10.1016/j.landurbplan.2013.04.009.
Green, S.M., Dungait, J.A.J., Tu, C., et al., 2019. Soil functions and ecosystem services research in the Chinese karst critical Zone[J]. Chem. Geol. 527, 119107. https://doi.org/10.1016/j.chemgeo.2019.03.018.
Halmy, M.W.A., Gessler, P.E., Hicke, J.A., Salem, B.B., 2015. Land use/land cover change detection and prediction in the north-western coastal desert of Egypt using markov-CA[J]. Appl. Geogr. 63, 101–112. https://doi.org/10.1016/j.apgeog.2015.06.015.
He, J.H., Pan, Z.Z., Liu, D.F., et al., 2019. Exploring the regional differences of ecosystem health and its driving factors in China[J]. Sci. Total Environ. 673 (JUL.10), 553–564. https://doi.org/10.1016/j.scitotenv.2019.03.465.
Howell, P.E., Muths, E., et al., 2018. Increasing connectivity between metapopulation ecology and landscape ecology[J]. Ecology 28. https://doi.org/10.1002/ecy.2189.
Ishtiaque, A., Myint, S.W., Wang, C., et al., 2016. Examining the ecosystem health and sustainability of the world's largest mangrove forest using multi-temporal MODIS products[J]. Sci. Total Environ. 569, 1241–1254. https://doi.org/10.1016/j.scitotenv.2016.06.200 (-).
Jiang, W.G., Yuan, L.H., Wang, W.J., Cao, R., Zhang, Y.F., et al., 2015. Spatio-temporal analysis of vegetation variation in the Yellow River Basin. Ecol. Indic. 51, 117–126. https://doi.org/10.1016/j.ecolind.2014.07.031.
Jiang, Z., Lian, Y., Qin, X., 2014. Rocky desertification in Southwest China: impacts, causes, and restoration. Earth-Sci. Rev. 132 (3), 1–12. https://doi.org/10.1016/j.earscirev.2014.01.005.
Jiang, Z.H., Liu, H.Y., Wang, H.Y., et al., 2020. Bedrock geochemistry influences vegetation growth by regulating the regolith water holding capacity[J]. Nat. Commun. https://doi.org/10.1038/s41467-020-16156-1.
Kang, P., Chen, W.P., Hou, Y., et al., 2018. Linking ecosystem services and ecosystem health to ecological risk assessment: a case study of the Beijing-Tianjin-Hebei urban agglomeration [J]. Sci. Total Environ. 636, 1442–1454. https://doi.org/10.1016/j.scitotenv.2018.04.427.
Keith, A.M., Schmidt, O., Mcmahon, B.J., 2016. Soil stewardship as a nexus between ecosystem services and one health[J]. Ecosyst. Serv. 17, 40–42. https://doi.org/10.1016/j.ecoser.2015.11.008.
Li, C.J., Bai, X.Y., Tan, Q., Luo, G.J., Wu, L.H., et al., 2022. High-resolution mapping of the global silicate weathering carbon sink and its long-term changes. Glob. Chang. Biol. 28, 4377–4394. https://doi.org/10.1111/gcb.16186.
Li, Y.R., Cao, Z., Long, H.L., 2017a. Dynamic analysis of ecological environment combined with land cover and NDVI changes and implications for sustainable urban rural development: the case of Mu Us Sandy Land, China. J. Clean. Prod. 142 (2), 697–715. https://doi.org/10.1016/j.jclepro.2016.09.011.
Li, F., Wang, W.J., Jiang, W.G., Chen, M., Wang, Y., 2017b. Spatio-temporal variations of vegetation cover and its responses to climate change in the Heilongjiang Basin of China from 2000 to 2014. Sci. Geogr. Sin. 37 (11), 1745–1754. https://doi.org/10.13249/j.cnki.sgs.2017.11.017.
Li, H.W., Wang, S.J., Bai, X.Y., et al., 2018. Spatiotemporal distribution and national measurement of the global carbonate carbon sink. Sci. Total Environ. 643 (DEC.1), 157. https://doi.org/10.1016/j.scitotenv.2018.06.196.
Li, Q., Shi, X.Y., Wu, Q.Q., 2020a. Exploring suitable topographical factor conditions for vegetation growth in wanhuigou catchment on the loess plateau, China: a new perspective for ecological protection and restoration. Ecol. Eng. 158, 106053. https://doi.org/10.1016/j.ecoleng.2020.106053.
Li, Q., Wang, S.J., Bai, X.Y., Luo, G.J., et al., 2020b. Change detection of soil formation rate in space and time based on multi source data and geospatial analysis techniques. Remote Sens. 12 (1), 121. https://doi.org/10.3390/rs12010121.
Li, Y.B., Wang, S.J., Wei, C.F., Long, J., 2006. The spatial distribution of soil loss tolerance in carbonate area in Guizhou province[J]. Earth Environ. 04, 36–40. https://doi.org/10.3969/j.issn.1672-9250.2006.04.007.
Li, Y.Y., An, Y.L., Yang, G.B., 2015. Dynamic evaluation of ecosystem health based on PSR model in Karst Areas——a case study of Guizhou Province[J]. Res. Soil Water Conserv. 22 (06), 279–286. https://doi.org/10.13869/j.cnki.rswc.2015.06.039.
Liao, C.J., Yue, Y.M., Wang, K.L., et al., 2018. Ecological restoration enhances ecosystem health in the karst regions of Southwest China. Ecol. Indic. 90, 416–425. https://doi.org/10.1016/j.ecolind.2018.03.036.
Liu, W.B., Sun, F.B., 2016. Assessing estimates of evaporative demand in climate models using observed pan evaporation over China[J]. J. Geophys. Res. Atmos. 121 (14). https://doi.org/10.1002/2016JD025166.
Lorencová, E.K., Harmáčková, Z.V., Landová, L., et al., 2016. Assessing impact of land use and climate change on regulating ecosystem services in the Czech republic[J]. Ecosyst. Health Sustain. 2 (3). https://doi.org/10.1002/ehs2.1210 n/a-n/a.
Lv, T.Y., Zeng, C., Lin, C.X., et al., 2023. Towards an integrated approach for land spatial ecological restoration zoning based on ecosystem health assessment[J]. Ecol Indic 147, 110016. https://doi.org/10.1016/j.ecolind.2023.110016.
Ma, Q.H., Zhang, K.L., 2018. Progress and prospect of soil erosion research in southwest karst area[J]. Adv. Earth Science 33 (11), 1130–1141.. https://kns.cnki.net/kcms/detail/detail.aspx?FileName=DXJZ201811004&DbName=CJFQ2018.
Madeira, C., Mendonça, V., Leal, M.C., et al., 2018. Environmental health assessment of warming coastal ecosystems in the tropics – application of integrative physiological indices[J]. Sci. Total Environ. 643, 28–39. https://doi.org/10.1016/j.scitotenv.2018.06.152.
Marco, A.D., Proietti, C., Anav, A., et al., 2019. Impacts of air pollution on human and ecosystem health, and implications for the National Emission Ceilings Directive: insights from Italy-NC-ND[J]. Environ. Int. 125, 320–333. https://doi.org/10.1016/j.envint.2019.01.064.
Marulli, J., Mallarach, J.M., 2005. A GIS methodology for assessing ecological connectivity: application to the Barcelona metropolitan area. Landsc. Urban Plan. 71 (2–4), 243–262. https://doi.org/10.1016/j.landurbplan.2004.03.007.
Mondal, M.S., Sharma, N., Garg, P.K., et al., 2016. Statistical independence test and validation of CA Markov land use land cover (LULC) prediction results[J]. Egypt. J. Remote Sens. Space. Sci., 259–272 https://doi.org/10.1016/j.ejrs.2016.08.001.
Pan, Z.Z., He, J.H., Liu, D.F., et al., 2020. Predicting the joint effects of future climate and land use change on ecosystem health in the middle reaches of the Yangtze River Economic Belt, China[J]. Appl. Geogr. 124, 102293. https://doi.org/10.1016/j.apgeog.2020.102293.
Pantus, F.J., Dennision, W., 2005. Quantifying and evaluating ecosystem health: a case study from Moreton Bay, Australia. Environ. Manag. 36 (5), 757–771. https://doi.org/10.1007/s00267-003-0110-6.
Peng, J., Liu, Y.X., Li, T.Y., Wu, J.S., 2017. Regional ecosystem health response to rural land use change: a case study in Lijiang City, China[J]. Ecol. Indic. 72, 399–410. https://doi.org/10.1016/j.ecolind.2016.08.024.
Peng, J., Liu, Y.X., Wu, J.S., et al., 2015. Linking ecosystem services and landscape patterns to assess urban ecosystem health: a case study in Shenzhen City, China[J]. Landsc. Urban Plan. 143, 56–68. https://doi.org/10.1016/j.landurbplan.2015.06.007.
Peterson, G.D., 2002. Contagious disturbance, ecological memory, and the emergence of landscape pattern[J]. Ecosystems 5 (4), 329–338. https://doi.org/10.1007/s10021-001-0077-1.
Phillips, L.B., Hansen, A.J., et al., 2008. Evaluating the species energy relationship with the newest measures of ecosystem energy: NDVI versus MODIS primary production [J]. Remote Sens. Environ. 112 (9), 3538–3549. https://doi.org/10.1016/j.rse.2008.04.012.
Plummer, L.N., Busenberg, E.B., 1982. The solubilities of calcite, aragonite and vaterite in CO2-H2O solutions between 0 and 90°C, and an evaluation of the aqueous model for the system CaCO3-CO2-H2O. Geochim. Cosmochim. Acta 46, 1011–1040. https://doi.org/10.1016/0016-7037(82)90056-4.
Qiu, B.K., Li, H.L., Zhou, M., Zhang, L., 2015. Vulnerability of ecosystem services provisioning to urbanization: a case of China. Ecol. Indic. 57, 505–513. https://doi.org/10.1016/j.ecolind.2015.04.025.
Ran, C., Wang, S.J., Bai, X.Y., et al., 2021. Evaluation of temporal and spatial changes of global ecosystem health[J]. Land Degrad. Dev. 32, 1500–1512. https://doi.org/10.1002/ldr.3813.
Reeves, M.C., Moreno, A.L., Bagne, K.E., et al., 2014. Estimating climate change effects on net primary production of rangelands in the United States[J]. Clim. Chang. 126 (3), 429–442. https://doi.org/10.1007/s10584-014-1235-8.
Roderick, M.L., Rotstayn, L.D., Farquhar, G.D., et al., 2007. On the attribution of changing pan evaporation[J]. Geophys. Res. Lett. 34 (17). https://doi.org/10.1029/2007GL031166.
Rombouts, I., Beaugrand, G., Artigas, L.F., et al., 2013. Evaluating marine ecosystem health: case studies of indicators using direct observations and modelling methods[J]. Ecol. Indic. 24, 353–365. https://doi.org/10.1016/j.ecolind.2012.07.001.
Sang, L., Zhang, C., Yang, J., et al., 2011. Simulation of land use spatial pattern of towns and villages based on CA–Markov model[J]. Math. Comput. Model. 54 (3–4), 938–943. https://doi.org/10.1016/j.mcm.2010.11.019.
Sen, P.K., 1968. Estimates of the regression coefficient based on Kendall's Tau[J]. Publ. Am. Stat. Assoc. 63 (324), 1379–1389. https://doi.org/10.1029/2022EF002746https://doi.org/10.1080/01621459.1968.10480934.
Seto, K.C., Satterthwaite, D., 2010. Interactions between urbanization and global environmental change[J]. Curr. Opin. Environ. Sustain. 2 (3), 127–128. https://doi.org/10.1016/j.cosust.2010.07.003.
Song, X.W., Gao, Y., Wen, X.F., et al., 2017. Carbon sequestration potential and its eco-service function in the karst area, China[J]. J. Geogr. Sci. 08, 73–86 https://doi.org/CNKI:SUN:ZGDE.0.2017-08-004.
Sun, C.X., Wang, S.J., Li, R.L., Li, Y.L., 2002a. Differential weathering and pedogenetic characteristics of carbonate rocksand their effect on the development of rock desertification in karst regions[J]. Acta Mineral. Sin. 04, 308–314. https://doi.org/10.1080/12265080208422884.
Sun, C.X., Wang, S.J., Liu, X.M., Feng, Z.G., 2002b. Geochemical characteristics of weathered shell rock-earth interface of carbonate rock and its formation process——take the limestone weathered shell profile of Huaxi, Guizhou Province as an example[J]. Acta Mineral. Sin. (02), 126–132 https://doi.org/10.1080/12265080208422884.
Sun, Y.J., Ren, Z.Y., et al., 2019. Spatial and temporal changes in the synergy and trade-off between ecosystem services, and its influencing factors in yanan, loess Plateau[J]. Acta Ecol. Sin. 39 (10), 3443–3454. https://doi.org/10.5846/stxb201808141730.
Turner, M.G., 1989. Landscape ecology: the effect of pattern on process[J]. Annu. Rev. Ecol. Syst. https://doi.org/10.1146/annurev.es.20.110189.001131.
Wang, P., Deng, X.Z., Zhou, H.M., et al., 2018. Responses of urban ecosystem health to precipitation extreme: a case study in Beijing and Tianjin. J. Clean. Prod. 177, 124–133. https://doi.org/10.1016/j.jclepro.2017.12.125.
Wang, S.J., 1999. Preliminary study on the weathering of carbonate rock[J]. Sci. China Ser. D Earth Sci. 29 (5), 442–449. https://doi.org/10.3321/j.issn:1006-9267.1999.05.008.
Wang, S.J., 2002. Concept deduction and its connotation of karst rocky desertification[J]. Carsologica Sin. 21 (2), 101–105. https://doi.org/10.1006/jfls.2001.0409.
Wang, Z.Y., Lin, Q., Zhao, Y.J., 2019. Problems related to weathering and pedogenesis of carbonate rock in karst area[J]. J. Guangxi Normal Univ. Nat. Sci. Ed. 036 (001), 94–99.. 10.16601/j.cnki.issn1001-8743.2019.01.019.
White, W.B., 1984. Rate processes: chemical kinetics and karst landform development. In: Lafleur, R.E. (Ed.), Groundwater as a Geomorphic Agent, Binghampton Symposia in Geomorphology. 13. Allen & Unwin, Boston , pp. 227–247.. https://www.researchgate.net/

publication/279706304_Rate_processes_chemical_kinetics_and_karst_landform_development.
Williams, C.H., Steinbergs, A., 1959. Soil sulphur fractions as chem-ical indices of available sulphur in some Australian soils[J]. Aust. J. Agric. Res. 10 (3), 340–352. https://doi.org/10.1071/AR9590340.
Wu, B., Qi, S., 2021. Effects of underlay on hill-slope surface runoff process of Cupressus funebris Endl. Plantations in Southwestern China. Forests 12 (5), 644. https://doi.org/10.3390/f12050644.
Xiao, Z., Liu, R., Gao, Y.H., et al., 2022. Spatiotemporal variation characteristics of ecosystem health and its driving mechanism in the mountains of southwest China[J]. J Clean Prod. 345, 131138. https://doi.org/10.1016/j.jclepro.2022.131138.
Xiao, B.Q., Bai, X.Y., Zhao, C.W., et al., 2023. Responses of carbon and water use efficiencies to climate and land use changes in China's karst areas[J]. J. Hydrol., 128968 https://doi.org/10.1016/j.jhydrol.2022.128968.
Xiao, R., Liu, Y., Fei, X., et al., 2019. Ecosystem health assessment: a comprehensive and detailed analysis of the case study in coastal metropolitan region, eastern China[J]. Ecol. Indic. 98 (MAR), 363–376. https://doi.org/10.1016/j.ecolind.2018.11.010.
Xie, X., Fang, B., Xu, H.Z., He, S.S., Li, X., 2021. Study on the coordinated relationship between urban land use efficiency and ecosystem health in China. Land Use Policy 102, 105235. https://doi.org/10.1016/j.landusepol.2020.105235.
Xiong, L., Bai, X.Y., Zhao, C.W., 2022. High-resolution datasets for global carbonate and silicate rock weathering carbon sinks and their change trends[J]. Earth's Future, e2022EF002746 https://doi.org/10.1029/2022EF002746.
Xu, Z.M., Huang, R.Q., Tang, Z.G., 2005. Research progress of formation mechanism of red soil overlying carbonate rocks in southern China[J]. Earth Environ. 33 (4), 29–36. https://doi.org/10.3969/j.issn.1672-9250.2005.04.005.
Yan, Y., Zhao, C., Wang, C., et al., 2016. Ecosystem health assessment of the Liao River basin upstream region based on ecosystem services:[J]. Acta Ecol. Sin. 36 (4), 294–300. https://doi.org/10.1016/j.chnaes.2016.06.005.
Yang, Y.J., Wang, S.J., Bai, X.Y., et al., 2019. Factors affecting long-term trends in global NDVI [J]. Forests 10 (5), 372. https://doi.org/10.3390/f10050372.
You, G.Y., Zhang, Y.P., Liu, Y.H., et al., 2013. On the attribution of changing pan evaporation in a nature reserve in SW China[J]. Hydrol. Process. 27 (18), 2676–2682. https://doi.org/10.1002/hyp.9394.
Yuan, D.X., 1988. On Karst environmental system[J]. Carsologica Sin. 1988 (03), 9–16 https://doi.org/CNKI:SUN:ZGYR.0.1988-03-002.
Yuan, D.X., 1997. Modern karstology and global change research[J]. Earth Sci. Front. 001, 17–25 https://doi.org/CNKI:SUN:DXQY.0.1997-Z1-003.
Zeng, C., Wang, S.J., Bai, X.Y., Li, Y.B., Tian, Y.C., Li, Y., Wu, L.H., Luo, G.J., 2017. Soil erosion evolution and spatial correlation analysis in a typical karst geomorphology using RUSLE with GIS. Solid Earth 8, 721–736. https://doi.org/10.5194/se-8-721-2017.
Zeng, S.B., Jiang, Y.J., Liu, Z.H., 2016. Assessment of climate impacts on the karst-related carbon sink in SW China using MPD and GIS[J]. Glob. Planet. Chang. 144, 171–181. https://doi.org/10.1016/j.gloplacha.2016.07.015.
Zhang, C., Yuan, D., 2005. IGCP448:progresses of world correlation of karst ecosystem[J]. Carsologica Sin. 24 (1), 83–88 https://doi.org/CNKI:SUN:ZGYR.0.2005-01-013.
Zhang, F.T., Su, W.C., Zhao, W.Q., 2011a. Ecosystem health assessment in mountainous areas of karst plateau based on ecological footprint model[J]. Bull. Water Soil Conserv. 31 (01), 256–261. https://doi.org/10.13961/j.cnki.stbctb.2011.01.022.
Zhang, X.B., Bai, X.Y., He, X.B., 2011b. Soil creeping in the weathering crust of carbonate rocks and underground soil losses in the karst mountain areas of Southwest china[J]. Carbonates Evaporites 26 (2), 149–153. https://doi.org/10.1007/s13146-011-0043-8.
Zhang, H.Q., Xu, E.Q., 2017. An evaluation of the ecological and environmental security on China's terrestrial ecosystems[J]. Sci. Rep. 7 (1), 811. https://doi.org/10.1038/s41598-017-00899-x.
Zhang, H.Y., Fan, J.W., Cao, W., et al., 2018. Changes in multiple ecosystem services between 2000 and 2013 and their driving factors in the grazing withdrawal program, China[J]. Ecol. Eng. 116, 67–79. https://doi.org/10.1016/j.ecoleng.2018.02.028.
Zhang, S.R., Bai, X.Y., Zhao, C.W., Tan, Q., Luo, G.J., 2021a. Limitations of soil moisture and formation rate on vegetation growth in karst areas. Sci. Total Environ. 6, 151209. https://doi.org/10.1016/j.scitotenv.2021.151209.
Zhang, Y.H., Xu, X.L., Li, Z.W., Xu, C.H., Luo, W., 2021b. Improvements in soil quality with vegetation succession in subtropical China karst. Sci. Total Environ. 775, 145876. https://doi.org/10.1016/j.scitotenv.
Zhang, X., Yue, Y.M., Tong, X.W., Wang, K.L., et al., 2021c. Eco-engineering controls vegetation trends in Southwest China karst. Sci. Total Environ. 770 (8), 145160. https://doi.org/10.1016/j.scitotenv.2021.145160.
Zhao, S., Pereira, P., Wu, X.Q., Zhou, J.X., et al., 2020. Global karst vegetation regime and its response to climate change and human activities. Ecol. Indic. 113, 106208. https://doi.org/10.1016/j.ecolind.2020.106208.